NMR study of copper with titanium impurities*

D. M. Follstaedt,† D. Abbas, T. S. Stakelon,‡ and C. P. Slichter
Materials Research Laboratory, University of Illinois, Urbana, Illinois 61801
(Received 21 January 1976)

We present results of an NMR study of copper containing titanium impurities. Satellites from a near-neighbor copper shell to the impurities were detected which possess a quadrupole coupling of $\nu_Q = 1.20 \pm 0.01$ MHz, asymmetry parameter $\eta \leq 0.08$, and magnetic shift $\Delta K/K = -0.23 \pm 0.01$. These values are compared with those of other $3d$ transition impurities in copper to show that the satellite is either a first neighbor, in which case η is unusually small, or a second neighbor. If the latter case is correct, the data show the spin density is reversed relative to its value at second neighbors to iron-group atoms at the right-hand side of the Periodic Table. We have observed first-order quadrupole "wings" whose positions are concentration dependent, and present a simple analysis of the "wings." We have measured the magnetic broadening of the ^{63}Cu main line at high fields. The data suggest that Ti impurities have a larger s-d exchange coupling J than Ni.

I. INTRODUCTION

The accepted theoretical description of $3d$ transition impurities in copper is that the d electrons are localized around the impurity site in virtual bound states.[1] Bulk measurements such as resistivity or magnetic broadening of the host NMR main line provide information about these impurity states only at the Fermi energy E_F, since they are asymptotic probes ($k_F r \gg 1$). To discover details of the virtual bound state below E_F, an experiment is needed which probes the conduction electrons scattered by the impurity at positions near the impurity ($k_F r \sim 1$).

Satellite NMR is such an experimental probe. Copper nuclei which are near neighbors to the impurity have their resonant positions shifted from the pure-copper position by magnetic hyperfine and electric quadrupole perturbations, with the conduction electrons scattered from the impurity. Their resonances appear as small satellites to the strong resonance from the abudant copper nuclei far from the impurity. Previous satellite studies have been reported on $3d$ elements in copper,[2-10] and other studies are presently underway.[11,12]

In this study of *Cu*Ti, we report satellite resonances of a shell of copper nuclei which are near neighbors of Ti impurities. We see a field-dependent satellite, and field-independent but concentration-dependent resonances which we refer to as "wings." We have measured the magnetic hyperfine and electric quadrupole couplings of the former. While one such satellite does not provide enough information to determine completely the width and position of the virtual bound state, it can be correlated with trends for other magnetic atoms. We have measured the magnetic broadening of the ^{63}Cu main line at high fields, and compared it with those of similar impurities.

In Sec. II we outline the experimental method. In Sec. III we discuss the field-dependent satellites, taking up the question of the shell of neighbors from which they originate. In Sec. IV we discuss the wings, and in Sec. V we discuss the width of the Cu main line.

II. EXPERIMENTAL METHOD

Samples were formed by arc melting a high-purity Cu rod with a chip of Ti of the appropriate weight. Details of this preparation have been given elsewhere.[8,10] Metallurgical studies[13] show that Ti is soluble in molten copper at the concentration used here ($c \leq 0.84$ at.%). Chemical analysis of three chips from each of the two alloys made gave average concentrations and variations of 0.143 ± 0.003 and 0.840 ± 0.030 at.%. Trace analysis gave <10 ppm concentration of any other element, and a total concentration of other $3d$ elements of <10 ppm.

The hybrid-junction NMR spectrometer used in this study has been extensively discussed elsewhere.[2,3] It is a phase-coherent apparatus in which the phase can be adjusted to pick out any linear combination of the complex susceptibility components χ'' and χ' (absorption and dispersion). The principal advantage of this capability over that of an apparatus which measures only χ'' is in enabling us to see small satellites obscured by the sloping tail of the absorption of the main line. By mixing χ' and χ'', the main-line tail can be flattened. Since all data are obtained using magnetic field modulation, the spectra displayed in the figures are derivatives of mixtures of χ' and χ''. Experiments were performed with frequencies ν_0 from 4.45 to 60.5 Mhz.

III. FIELD-DEPENDENT SATELLITES

If the resonance is observed at a fixed frequency ν_0, the splitting ΔH of a satellite from the main line may arise from three interactions: (i) a magnetic splitting with $\Delta H \propto \nu_0$, (ii) a first-order quadrupole coupling with ΔH independent of ν_0, and (iii) a second-order quadrupole coupling with $\Delta H \propto \nu_0^{-1}$. Thus in general

$$\Delta H = a\nu_0 + b + c/\nu_0 . \quad (1)$$

For the $(+\frac{1}{2}, -\frac{1}{2})$ transition, which is most frequently what one sees for a satellite, $b = 0$ (no first-order quadrupole shift). If $b \neq 0$ one expects $b \gg c/\nu_0$ for the site couplings we encounter.

At low fields $c/\nu_0 \gg a\nu_0$ (second-order quadrupole coupling dominates the magnetic shift), so that a plot of ΔH vs $1/\nu_0$ is a straight line at low frequencies, but deviates at high frequency. A plot of $\nu_0 \Delta H$ vs ν_0^2, which gives a straight line for all frequencies if $b = 0$, provides a simple test of Eq. (1) with $b = 0$.

For an individual nuclear neighbor of the magnetic atom, the coefficients a, b, and c depend on the orientations of the static field H_0 with respect to the crystalline axes. Often a is nearly independent of orientation but b and c are strongly dependent on orientation. Thus, for a powder sample, the shift ΔH is smeared over a continuum. However, the powder pattern has peaks in its absorption intensity which show up as features in the derivative spectrum. We label these peaks A, B, etc.

Figure 1 shows a satellite labeled A at 7.9 MHz and 4.2 K. Its position depends on the magnetic field but is independent of the Ti concentration. Figure 2 shows a feature we label a wing. Its position is independent of H_0 but depends on the Ti concentration of the sample.

Figure 3(a) compiles the position of satellites and wings in the 0.14-at.%-Ti sample. It plots ΔH vs $1/\nu_0$. Figures 3(b) and 3(c) are plots of $\nu_0 \Delta H$ vs ν_0^2 for satellites A and B from the same sample. Figure 4 gives ΔH vs $1/\nu_0$ for the 0.84-at.%-Ti sample. In Figs. 3(a) and 4 the dashed straight line shows the $1/\nu_0$ second-order quadrupole variations at low frequency. Note that frequency-independent wings (C, D, E, and F) are observed in both samples, but occur at different values of ΔH.

Comparison with data from other systems shows that A and B arise from satellites which are near neighbors of the Ti, as they are produced by nuclei close enough to the Ti impurity to have second-order quadrupole shifts at low frequencies ($\Delta H \propto \nu_0^{-1}$) and to have magnetic shifts at high frequencies ($\Delta H \propto \nu_0$). Both dependences are observed in the wide range of frequencies studied, 4.45 (~4kG) to 60.5 Mhz (~53kG). As we shall explain, A and B are two features of the powder pattern of a single shell of neighbors, the first or the second, and correspond to axial symmetry as best we can tell.

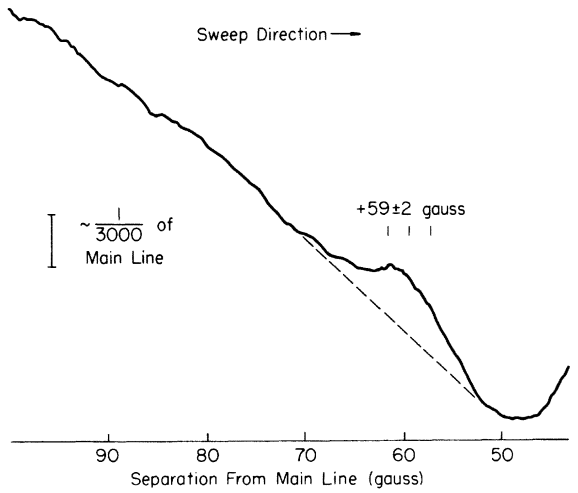

FIG. 1. Satellite A at 7.9 MHz, 4.2 K in the Cu–0.14-at. %-Ti sample. Modulation amplitude is set to give maximum ^{63}Cu main-line signal without additional broadening. Data are the derivative of a mixture of absorption and dispersion (since a slight amount of χ' has been added to the predominantly χ'' phase) vs separation from the ^{63}Cu main line. Trace shown is the signal-averager output of 42 sweeps with a 1-sec lock-in time constant.

A. Determination of the magnetic and quadrupole coupling parameters

Satellite A is seen at all fields and corresponds to the high-field edge of a second-order quadrupole

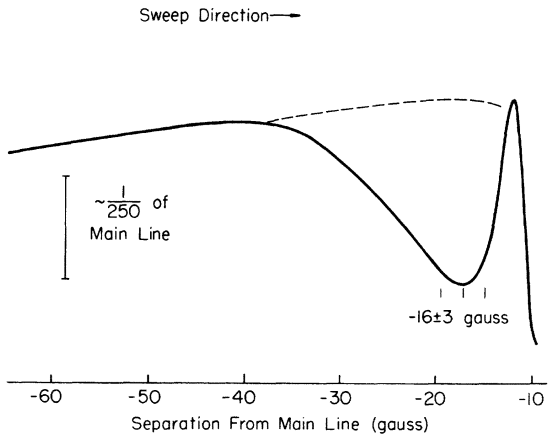

FIG. 2. Wing D at 7.9 MHz, 4.2 K in the Cu–0.14-at. %-Ti sample. Modulation amplitude set to give maximum signal without broadening. Phase contains small amount of χ' to give optimum baseline. Trace shown is the signal averager output of 33 sweeps with a 1-sec lock-in time constant.

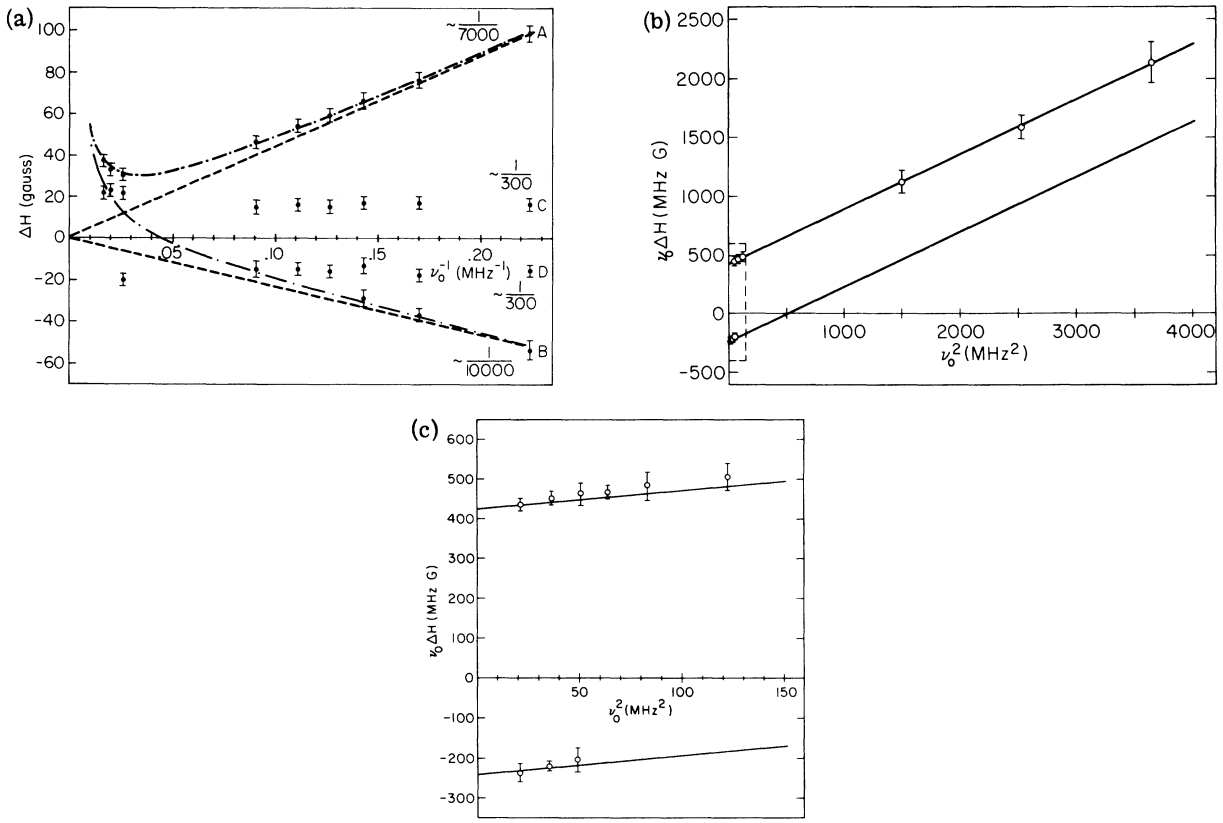

FIG. 3. (a) Resonance spectrum of Cu–0.14-at.%-Ti sample. Splittings are relative to the ^{63}Cu main-line position (shifts to higher fields plotted as positive ΔH). The numbers give the intensity as a fraction of that of the main line. Data at low fequencies, $\nu_0 < 11$ MHz or $H_0 < 10$ kG, were obtained at 4.2 K; high-frequency data at ~300 K. The dashed lines show the ν_0^{-1} quadrupole dependence at low frequencies. The dash-dot line is the least-squares fit discussed in the text. (b) Replot of the field-dependent data of (a) as $\nu_0\Delta H$ vs ν_0^2, which should theoretically be a straight line. The solid lines represent the parameters given in the text. (c) Expanded replot of the low-frequency data (dashed area) of (b).

powder pattern with a superimposed magnetic shift (a very similar powder pattern and field dependence was observed[3] for *Cu*Ni). A typical observation is shown in Fig. 1. We make small corrections (~ – 1.5 G) in the splitting of A according to the computer-calculated dipolar-broadened second-order powder patterns found by Baughier *et al.*[14] in order to obtain the unbroadened pattern's edge. A least-squares fit to these corrected data gives

$$\Delta H_A = 0.468\nu_0 + 425/\nu_0 , \qquad (2)$$

where ΔH_A is given in G and ν_0 in MHz. The magnetic-shift value is determined principally by the high-field data at 300 K, although the magnetic shift is non-negligible at 10 kG, for data taken at 4.2 K. However, similar shifts in *Cu*V (Ref. 10) changed only ~7% between these temperatures; the *Cu*Ti change is expected to be less. If we normalize the satellite shift (ΔK) to the Knight shift of pure copper ($K = 0.232\%$), we obtain $\Delta K/K = -0.23$

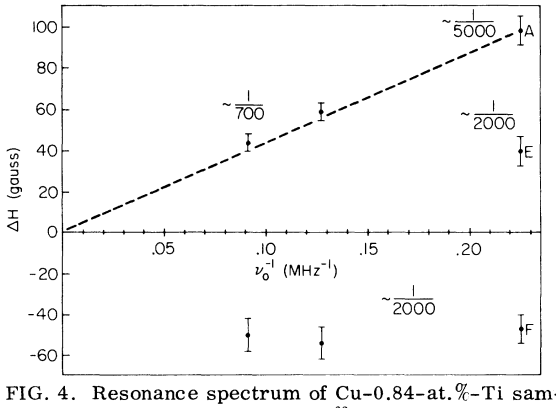

FIG. 4. Resonance spectrum of Cu-0.84-at.%-Ti sample. Splittings are relative to the ^{63}Cu main-line position (shifts to higher fields plotted as positive ΔH) and intensity fractions relative to its intensity. Data obtained at 4.2 K. Dashed line shows the ν_0^{-1} dependence of satellite A observed at low frequencies in the 0.14-at.%-Ti sample. Position of the wings in this sample is ~±45 G, though their large width makes exact determination difficult.

±0.01.

Second-order patterns also have singularities on their low-field side, with a splitting from the pattern center ~$\frac{9}{16}$ that of the high-field singularities for an axially symmetric field gradient. The low-field singularities are of comparable intensity and should also be detectable. Satellite B meets all of these requirements and is taken to be part of the same pattern as A. It is seen only below 7 MHz; above 7 MHz it is obscured by resonances D and C and the main line. At sufficiently high ν_0 satellite B should merge with A. It should have the same magnetic coupling term $a\nu_0$ as A and $-\frac{9}{16}$ the c/ν_0 term, and hence should fit the relation

$$\Delta H_B = 0.468\nu_0 - 239/\nu_0 . \quad (3)$$

This curve is also shown in Fig. 3 and clearly fits the data well. Observe that for $\nu_0^{-1} > 0.12$, B is lost under the main line. Figures 3(b) and 3(c) ($\nu_0 \Delta H$ vs ν_0^2) compare the data in a straight-line plot.

For nonzero asymmetry parameter (η), the high-field singularity splits into two singularities whose distances from the main line are proportional to $1-\eta$ and $1+\eta$. Since we see no splitting, η must be approximately zero (see below). We have searched with adequate sensitivity to observe a second resonance on the high-field side, but are unable to find one.

Note that we can reject the alternate interpretation that the high-field singularity is *widely* split and that we missed one of the lines, requiring $\eta > 0.32$, since for such a large η the low-field singularity splits also, contrary to observation, and the A to B splitting ratio would not be $\frac{16}{9}$.

We are led to the conclusion that if the powder pattern has $\eta \neq 0$, the splitting of the high-field singularities must be less than the width of the observed dipolar-broadened resonance. The low-frequency data provide the most stringent requirements on η. At 7.0 MHz, the linewidth and signal-to-noise ratio give the requirement $\eta < 0.08$. Fitting the quadrupole term of the observed splitting to the singularity position for an $\eta = 0$ powder pattern gives $\nu_Q = 1.20 \pm 0.01$ MHz, or $q = 4.39 \pm 0.04 \times 10^{23}$ cm^{-3}.

B. Identification of the shell producing the satellites

We wish to deduce which shell of copper nuclei around the titanium impurity is producing the powder pattern resonances, A and B. For our powder samples we can make use of the observed parameters ν_Q, η, and $\Delta K/K$, together with data on the magnetic susceptibility χ, and their comparison with values in other Cu-based alloys for which single-crystal studies give unambiguous identification of which shell is involved. Such comparisons give only two possibilities for the shell; the first or the second neighbor. Let us give the reasoning.

1. ν_Q

Table I lists the known ν_Q's and η's for Cu-based alloys for first- and second-neighbor shells.

The size of our quadrupole coupling ($\nu_Q = 1.20 \pm 0.01$ MHz) is comparable to those determined for first or second neighbors to other impurities in copper. Since ν_Q is thought to decrease roughly with distance from the impurity r as the product of r^{-3} times an oscillatory function of r, the powder pattern is less likely to be due to more distant neighboring shells. The value would fit nicely among the first-neighbor ν_Q's. If the second-neighbor assignment is correct, only two other impurities[15] (Sn: $\nu_Q = 1.16$ MHz; Sb: $\nu_Q = 1.74$ MHz) have couplings as large at second-neighbor sites. For no other impurity does the first-neighbor ν_Q exceed that of the second. The absence of third-neighbor observations shows that such distant

TABLE I. ν_Q (MHz) and η for Cu-based alloys.

	First neighbor			Second neighbor			Fourth neighbor		
		η	Reference	ν_Q	η	Reference	ν_Q	η	Reference
Mn				0.280	0	11	0.188	0.65	11
Co	0.376	0.44	9						
Ni	1.120	0.20	9, 15, 24						
Zn	1.960	0.265	24	0.090	0	25			
Ge	1.940	0.905	15						
Ag	0.570	0.75	24	0.475	0	24			
Cd	1.520	0.036	24	0.410	0	24			
In	2.200	0.32	15	<0.800	0	15			
Sn	2.300	0.64	15	1.160	0	15			
Sb	2.600	0.75	15	1.740	0	15			
Au	2.650	0.05	24	0.823	0	24			

couplings do not produce large enough second-order shifts to be observed.

For the systems seen in Table I, a and c [Eq. (1)] are larger for the first-neighbor shell than the corresponding a and c of the second shell. Thus in some instances (e.g., CuNi) only the first neighbor is split enough either at low or high fields to be seen. We may thus ask if this is the second neighbor, where is the first neighbor?

There are two possibilities. The first is that the oscillatory nature of both magnetic and electric couplings with distance from the impurity has a phase which overcomes the roughly $1/r^3$ effect, making the first-neighbor a and c smaller than the corresponding a and c of the second neighbor.

The other alternative is that the first-shell quadrupole coupling smears the low-frequency resonance too broadly to be detected, and that at high-frequency the magnetic anisotropy smears the line too broadly to be seen. We think this alternative unlikely, however, since we have seen the high-field magnetic splittings of Mn, Fe, and Co first and second neighbors, atoms which are seen to be much more magnetic that Ti from the susceptibility measurements. Thus we are observing either a first neighbor or a second neighbor which has bigger magnetic and quadrupole splittings than the first.

2. η

For the second shell, symmetry requires $\eta = 0$, since the Cu-Ti axis possesses fourfold symmetry. For first neighbors the twofold axis permits $\eta \neq 0$. We see from Table I on Cu-based alloys that of the ten first neighbors studied only Cd ($\eta = 0.036$) and Au ($\eta = 0.05$) have η less than our upper limit of 0.08, whereas eight (Co, Ni, Zn, Ge, Ag, In, Sn, and Sb) have substantially larger η. This suggests that an η as small as we require probably does not come from a first neighbor.

Thus either the satellites represent a second neighbor with $\eta = 0$ or there is some factor which makes η much smaller than it is in $\frac{3}{4}$ of the other Cu-based alloys which have been studied.

C. Susceptibility χ and $\Delta K/K$

One method of identifying the satellite is to look for systematic variation of $\Delta K/K$ across the iron group for identified satellites of copper neighbors of iron-group impurities. Most theories of the spin density make $\Delta K/K$ proportional to the susceptibility χ. [We here assume χ arises largely from the spin of the magnetic ion, with a proportionality factor which depends on the ion. For example, the Ruderman-Kittel-Kasuya-Yosida (RKKY) expressions give a polarization proportional to $\chi_i J$, where the exchange coupling constant J depends on the ion.] Since χ varies by nearly two orders of magnitude across the iron group, we have plotted $\Delta K/K\chi$ in Fig. 5 using the susceptibilities given in Table II.

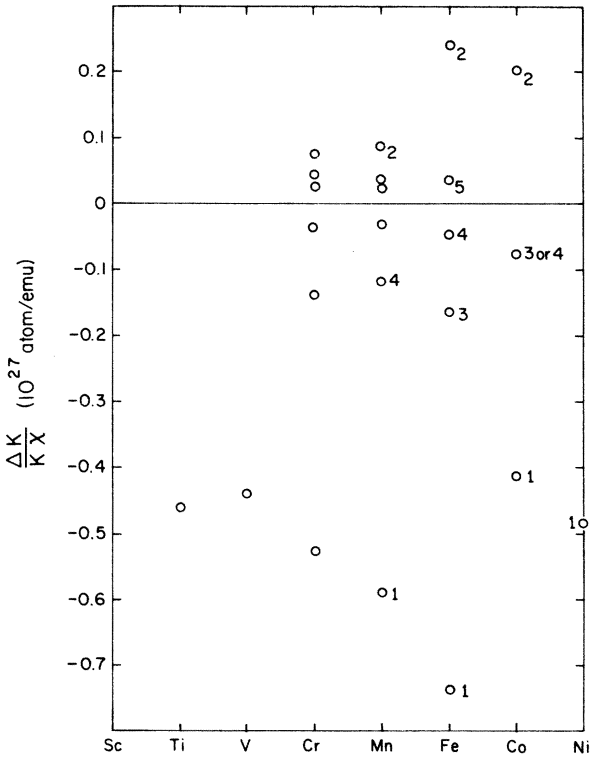

FIG. 5. $\Delta K/K\chi$ for various iron group magnetic atoms in copper, summarizing the results on $\Delta K/K$ found by the authors and their colleagues at the University of Illinois. The symbols 1–5 refer to the shell (first neighbor, second neighbor, etc., of the magnetic atom) where positive identification has been possible. One Sc satellite has been seen but is not plotted, since χ is not known for CuSc. Since the $\Delta K/K$ values are usually more reliable than the values of χ, the precision of comparisons between different magnetic atoms is limited by the data on χ.

For Ni, Co, Fe, and Mn the satellites arising

TABLE II. Susceptibility of Cu-based alloys.

Impurity	χ (10^{-27} emu/atom)	Reference
Ti	0.5	26
V	1.5	26
Cr	10.6	27
Mn	16.6	27
Fe	7.28	28
Co	4.0	29
Ni	0.24	30

from the first shell of neighbors have been positively identified. The data clearly suggest which satellites are the first neighbors for V and Cr, because of the smooth variation of $\Delta K/K\chi$ which that assignment would imply. The identified first-neighbor shifts would naturally lead one to assigning the Ti satellite to the first-neighbor position. However, examination of the second neighbor of Co, Fe, and Mn shows there is the possibility that the second-neighbor $\Delta K/K$ has become negative at Ti. This trend would be consistent with the Cr data for which the most positive $\Delta K/K\chi$ is 0.0679×10^{27}. Moreover, Follstaedt[10,16] gives arguments to support assignment of the V satellite to the second shell, which would then favor a second-shell assignment for Ti. We therefore conclude from $\Delta K/K\chi$ that the satellite may be either the first or second neighbor.

D. Conclusions

The data are easily reconciled with the satellite arising from the first shell, except for the anomously small asymmetry parameter η. The satellite could be a second neighbor, in which case the second-neighbor $\Delta K/K$ has a sign change relative to its value on the right-hand side of the iron group.

E. Evidence for a magnetic structure change

Aton[11] has called our attention to the smooth variation of $\Delta K/K\chi$ between V and Fe, with the large jump between Fe and Co. He suggests that this may indicate a change in magnetic structure. As a possibility he suggests that Co is nonmagnetic in the Anderson sense (no permanent moment, no splitting of the spin-up spin-down resonance in the absence of an applied static field). Of course, there may be other explanations. Probably the precision with which susceptibilities are known, together with the uncertain identification, do not permit a similar conclusion concerning Ti.

IV. DISCUSSION OF THE WING RESONANCES

A. General considerations

In the Cu–0.14-at.%-Ti sample we observed field-independent wings at $\Delta H = \pm 16$ G. In the Cu–0.84-at.%-Ti sample field-independent wings were observed at ± 45 G. Similar field-independent but concentration-dependent lines have been observed in CuNi alloys as well. The field independence suggests they represent first-order quadrupole splittings. The concentration dependence, however, is a mystery. We turn now to a possible explanation.

If we could observe the NMR of the Cu neighbors of a single isolated Ti atom, we would expect to get first-order satellites from each shell of neighbors. Roughly speaking, the farther the neighbors, the smaller the splitting. The near neighbors would thus have lines far from the main line. These resonances would exist as a smear in a powder.

In a sample of concentration c, each impurity has about $1/c$ atoms which are nearer to it than any other impurity. We can approximate this by saying that those atoms lie within a sphere of radius r_c. Clearly $r_c^3 \propto 1/c$. Hence as the concentration is increased r_c decreases. The observation of a neighbor resonance implies that the radius r_j of the shell producing it satisfies $r_j < r_c$. If the resonance disappears with increasing concentration, we presume that r_c has decreased until $r_c < r_j$, or that it is no longer meaningful to discuss the jth-neighboring shell at this higher concentration. Knowing the concentration at which the resonance disappears then gives an indication of which neighboring shell produced it at dilute concentrations.

Only those neighbor resonances which have sufficient nuclei to be seen at a concentration low enough to satisfy the $r_j < r_c$ criterion are observed. Thus more distant shells, which can satisfy $r_j < r_c$ only at low concentration, require many atoms to be seen.

Moreover, since these lines have first-order quadrupole splittings, they are subject to first-order wipeout. Their intensity thus peaks at a concentration $c \sim 1/n_w$, where n_w is the first-order wipeout number. Since $n_W \sim 1000$ and we are using $c > 0.1$ at.%, wipeout effects are definitely affecting wing intensities.

B. Application to Cu-Ti wings

The wings at ± 16 G were seen in the 0.14-at.%-Ti sample, giving $n = c^{-1} = 714$. The neighborhood sphere thus includes shells through the twenty-third. (Reference 17 lists the number of nuclei in the nearest fifty shells.) These wings have disappeared at a concentration of 0.84-at.% Ti, or $n_c = 119$, with a neighborhood extending to approximately the seventh shell. Presumably any shell between these could be considered to have produced the wings. Some will be more probable than others due to their increased number of shell members (n_i). It is also possible that more than one shell contributes to the wings. In the asymptotic limit, quadrupole couplings are expected to be approximately

$$\nu_Q \propto \cos(2k_F r + \phi)/r^3 .$$

If two (or more) shells differ an amount Δr such that $\Delta r < (2k_F)^{-1}$, their quadrupole shifts may be approximately equal, so that they contribute to the same wing. Without a more detailed concentration analysis, we cannot more accurately specify which shell

produces the wings.

The wings at ±45 G in the 0.84-at.%-Ti sample are not observed in the 0.14-at.%-Ti sample, evidently due to weaker intensity. They come from a shell which is closer than the seventh.

C. Application to Cu-Ni wings

Similar concentration-dependent wings were also observed in *Cu*Ni. In a Cu–0.10-at.%-Ni sample, first-order quadrupole wings were observed at ±30 G.[18] The concentration shows that they are within approximately the twenty-eighth shell. When the Ni concentration is increased to 0.54 at.%, they disappear.[3] Hence they must be more distant than approximately the tenth shell. With this large number of possible shells, it is again too difficult to speculate which shells produced the wings.

In samples with 0.54- and 0.71-at.% Ni, wings were observed at ±15 G.[3] The higher concentration places the outermost neighborhood shell at ~8. When the concentration was increased to 1.5-at.% Ni, these wings disappeared,[18] which places the shell producing them beyond about the fourth shell. The shell with the most members in this range is the seventh (48 members), and is perhaps the most likely to be producing the wings.

With a concentration of 1.5-at.% Ni, wings become present at ~±25 G.[18] At this concentration, wipeout is severest ($r_c \ll r_w$); also, the data taken by Lo *et al.*[3] were at ~7 kG, and the splittings are comparable to those of the second-order powder pattern of the first neighbors. The data at this concentration are hence the least likely to be adequately treated by our model, which places the origin of the wings stemming from neighbors no more distant than about the fourth shell.

We can also compare the first-order wing splittings with quadrupole resonances observed in *Cu*Ni by Whalley and Slichter.[6] Their resonance with $\nu_Q = 40$ kHz predicts a powder pattern edge at $\sim \frac{1}{2}\nu_Q(2\pi/\gamma) = 18$ G. This is close to the wing in the 0.54- and 0.71-at.%-Ni samples thought to stem from about the seventh shell.

V. WIDTH OF THE Cu MAIN LINE

We have observed the broadening of the ^{63}Cu main line at high fields and 300 K for the Cu–0.14-at.%-Ti sample. The linewidth is 9.3 ± 0.5 G at 60.4 MHz (53.4 kG), decreasing monotonically to the pure-copper width (6.7 G) at low fields.

For a comparison with other transition-metal impurities we use RKKY theory, following the procedure previously used for[2] *Cu*Co and[10] *Cu*V. The work of Sugawara is used to deconvolute the magnetic broadening due to RKKY-like conduction-electron magnetization oscillations around distant impurities from the nuclear dipole broadening. At 53.4 kG, the magnetic width is the same as the dipolar width; assuming a Lorentzian magnetic-broadening function, the half-width is $\Delta = 3.3$ G.

We use the theory of Walstedt and Walker[19] to compute A in the assumed RKKY broadening function

$$\Delta H(r) = (A/r^3)\cos(2k_F r + \phi).$$

They find

$$\Delta = 16\pi A c/3a^3,$$

where c is the impurity concentration and a is the bcc lattice constant (3.61 Å for Cu). In the RKKY theory A is proportional to χJ, where J is the s-d exchange coupling. At 53.4 kG we have $A = 6600$ G Å^3.

This value is the same as that estimated by Lang *et al.*[2] for isolated Co impurities and slightly larger than that obtained for *Cu*V (5000 G Å^3).[12,20] Several factors hinder the comparison of Ti, V, and Co impurities. While Co is soluble in molten Cu up to several percent,[13] the analysis of Lang *et al.*[2] depends upon the separation of the magnetic broadening into contributions from isolated Co atoms and other clusters of Co atoms, which they show must exist. V is barely soluble (~0.1 at.%).[13] Its dissolved concentration can be estimated,[12,20] but some evidence is also found for clustering. Finally, the actual broadening of the Ti and V samples is only slightly greater than the pure-copper width and the above numbers must be accepted as estimates. Hence we do not believe the above data are accurate enough to make detailed comparison between such close values.

We have also examined the main-line width obtained by Lo *et al.*[3,20] on a Cu–0.71-at.%-Ni sample. At 66 MHz (58.4 kG) the width is 8.6 ± 1.0 G, giving $\Delta \approx 2.25$ G and $A \approx 900$ G Å^3. Since Ni forms a random solid solution in Cu and Ti is soluble in Cu at our concentration (0.14 at.%), the analyzed impurity concentrations are indicative of the isolated impurity concentrations. Even with the small broadening widths, it is acceptable to assume that Ti impurities are more effective magnetic broadeners than Ni, by perhaps as much as a factor of ~6. Since the susceptibility of Ti is only twice that of Ni, we conclude the s-d exchange is larger in Ti than Ni.

Regardless of exact neighbor identification, we note that satellite shift, susceptibility, and magnetic linewidth broadening comparisons suggest that Ti impurities are more magnetic than Ni. However, as free atoms, both have two unpaired electrons. These impurities have two 4s electrons, versus one 4s electron for copper. A possible

explanation of the above magnetic comparison is that the 3*d* virtual bound state acquires part or all of the second 4*s* electron, giving Ti more than two 3*d* electrons and Ni less than two 3*d* holes. Analysis of residual resistivity, quadrupole wipeout, magnetic susceptibility, and thermoelectric power in *Cu*Ni (Refs. 21 and 22) give nine 3*d* electrons (one 3*d* hole), in agreement with optical-absorption measurements.[23] Similar bulk measurements of conduction electron scattering[22] in *Cu*Ti yield three 3*d* electrons. Thus analysis of these measurements supports our conjecture.

---

*Research supported in part by the U. S. Energy Research and Development Administration under Contract No. ERDA (11–1)–1198.

†Present address: Division 5151, Sandia Laboratories, Albuquerque, N. M. 87115.

‡Present address: Physics Department, Ohio State University, Columbus, Ohio 43210.

[1]E. Daniel and J. Friedel, in *Proceedings of the Ninth International Conference on Low Temperature Physics*, edited by J. G. Daunt, D. O. Edwards, F. J. Milford, and M. Yaqub (Plenum, New York, 1965), Pt. B, p. 933.

[2]D. V. Lang, J. B. Boyce, D. C. Lo, and C. P. Slichter, Phys. Rev. B 9, 3077 (1974); Phys. Rev. Lett. 29, 766 (1972).

[3]D. C. Lo, D. V. Lang, J. B. Boyce, and C. P. Slichter, Phys. Rev. B 8, 973 (1973).

[4]N. Karnezos and J. A. Gardner, Phys. Rev. B 9, 3106 (1974).

[5]J. Boyce, T. Aton, T. Stakelon, and C. P. Slichter, in Proceedings of the Fifth International Symposium on Magnetic Resonance, 1974 (unpublished); J. Boyce, T. Aton, and C. P. Slichter, AIP Conf. Proc. 18, 252 (1974).

[6]L. R. Whalley and C. P. Slichter, Phys. Rev. B 9, 3793 (1974).

[7]J. B. Boyce and C. P. Slichter, Phys. Rev. Lett. 32, 61 (1974).

[8]J. B. Boyce, Ph.D. thesis (University of Illinois, 1972) (unpublished).

[9]T. Stakelon, Ph.D. thesis (University of Illinois, 1974) (unpublished).

[10]D. Follstaedt, Ph.D. thesis (University of Illinois, 1975) (unpublished).

[11]T. Aton (private communication).

[12]D. Abbas (private communication).

[13]F. A. Schunk, *Constitution of Binary Alloys, Second Supplement* (McGraw-Hill, New York, 1969), p. 296.

[14]J. F. Baughier, H. M. Kriz, P. C. Taylor, and P. J. Bray, J. Magn. Reson. 3, 415 (1970).

[15]B. L. Jensen, R. Nevald, D. Ll. Williams, J. Phys. F 2, 169 (1972).

[16]D. Follstaedt and C. P. Slichter (unpublished).

[17]J. M. Brettell and A. J. Heeger, Phys. Rev. 153, 319 (1967).

[18]D. V. Lang (private communication).

[19]R. E. Walstedt and L. R. Walker, Phys. Rev. B 9, 4857 (1974).

[20]We wish to thank the authors of Ref. 3 for making their raw data available to us for further analysis.

[21]M. T. Béal-Monod, Phys. Rev. 164, 360 (1967).

[22]E. Brewig, W. Kierspe, U. Schotte, and D. Wagner, J. Phys. Chem. Solids 30, 483 (1969).

[23]H. D. Drew and R. E. Doezema, Phys. Rev. Lett. 28, 1581 (1972).

[24]G. Schnackenburg and R. T. Schumacher, Phys. Rev. B 7, 2292 (1973).

[25]A. G. Redfield, Phys. Rev. 130, 589 (1973).

[26]W. D. Weiss, Z. Metallkd. 58, 895 (1967).

[27]M. D. Daybell and W. A. Steyert, Rev. Mod. Phys. 40, 380 (1968).

[28]J. L. Tholence and R. Tournier, Phys. Rev. Lett. 25, 867 (1970).

[29]R. Tournier and A. Blandin, Phys. Rev. Lett. 24, 397 (1970).

[30]E. W. Pugh, B. R. Coles, A. Arrott, and J. E. Goldman, Phys. Rev. 105, 814 (1957).